THE JOURNAL OF BIOLOGICAL CHEMISTRY VOL. 287, NO. 24, pp. 20290–20300, June 8, 2012

Monospecific Inhibitors Show That Both Mannan-binding Lectin-associated Serine Protease-1 (MASP-1) and -2 Are Essential for Lectin Pathway Activation and Reveal Structural Plasticity of MASP-2*[S]

Received for publication, February 17, 2012, and in revised form, March 30, 2012 Published, JBC Papers in Press, April 16, 2012, DOI 10.1074/jbc.M112.354332

Dávid Héja[‡1,2], **Veronika Harmat**[§¶1], **Krisztián Fodor**[**], **Matthias Wilmanns**[**], **József Dobó**[‖3], **Katalin A. Kékesi**[‡‡§§], **Péter Závodszky**[‖], **Péter Gál**[‖4,5], **and Gábor Pál**[‡3,4,6]

From the [‡]*Department of Biochemistry, Eötvös Loránd University, 1/C Pázmány Péter Street, H-1117, Budapest, Hungary,* [§]*Institute of Chemistry, Eötvös Loránd University, 1/A Pázmány Péter Street, H-1117, Budapest, Hungary,* [¶]*Protein Modeling Research Group, Hungarian Academy of Sciences, Eötvös Loránd University, 1/A Pázmány Péter Street, H-1117, Budapest, Hungary,* [**]*European Molecular Biology Laboratory-Hamburg, c/o DESY, Building 25a, Notkestrasse 85, 22603 Hamburg, Germany,* [‖]*Institute of Enzymology, Research Centre for Natural Sciences, Hungarian Academy of Sciences, 29. Karolina street, H-1113, Budapest, Hungary,* [‡‡]*Department of Physiology and Neurobiology of Eötvös Loránd University, 1/C Pázmány Péter Street, H-1117, Budapest, Hungary, and* [§§]*Proteomics Group of the Biology Institute of Eötvös Loránd University, 1/C Pázmány Péter Street, H-1117, Budapest, Hungary*

Background: MASP-1 is considered as auxiliary, whereas MASP-2 is considered as a key protease in lectin-pathway activation.
Results: MASP-1 inhibitor SGMI-1 and MASP-2 inhibitor SGMI-2 completely block lectin pathway activation; the MASP-2·SGMI-2 complex reveals structural plasticity.
Conclusion: MASP-1 is a key component; MASP-2 functions through induced fit or conformational selection.
Significance: The lectin pathway activation model is incorrect. SGMIs revolutionize studying and enable regulating the lectin pathway.

The lectin pathway is an antibody-independent activation route of the complement system. It provides immediate defense against pathogens and altered self-cells, but it also causes severe tissue damage after stroke, heart attack, and other ischemia reperfusion injuries. The pathway is triggered by target binding of pattern recognition molecules leading to the activation of zymogen mannan-binding lectin-associated serine proteases (MASPs). MASP-2 is considered as the autonomous pathway-activator, while MASP-1 is considered as an auxiliary component. We evolved a pair of monospecific MASP inhibitors. In accordance with the key role of MASP-2, the MASP-2 inhibitor completely blocks the lectin pathway activation. Importantly, the MASP-1 inhibitor does the same, demonstrating that MASP-1 is not an auxiliary but an essential pathway component. We report the first Michaelis-like complex structures of MASP-1 and MASP-2 formed with substrate-like inhibitors. The 1.28 Å resolution MASP-2 structure reveals significant plasticity of the protease, suggesting that either an induced fit or a conformational selection mechanism should contribute to the extreme specificity of the enzyme.

The complement system has three activating routes, the classical, the alternative, and the lectin pathway. These are triggered by distinct danger signals and are involved in different pathologies (1). The three pathways culminate in the same effector route in a cascade like process in which associated zymogen proteases are activated and several key protein components are cleaved. The alternative route provides a positive feedback loop for all activation routes. Pathway-selective inhibitors would be excellent research tools to dissect the individual roles of each pathway in physiology and pathology. Such inhibitors could also lead to highly potent drugs that block only the pathology-related activation route while letting the other two fulfill their vital functions.

The lectin pathway is the most recently discovered and apparently the most complex complement pathway (2). It has at least five different pattern recognition molecules: mannan-binding lectin (MBL),[7] three types of ficolins (L, H, and M), and collectin 11 (3). Some of these recognition molecules can assume different oligomeric states, and there are

* This work was supported by the Hungarian Scientific Research Fund (OTKA) NK81950, K68408, NK100769 (to G. P.), NK77978 and NK100834 (to P. G.), and F67937, NK67800 and K72973 (to V. H.) as well as by Ányos Jedlik Grant NKFP_07_1-MASPOK07, NDA Grant KMOP-1.1.2-07/1-2008-0003, and European Union and the European Social Fund (TÁMOP) 4.2.1./B-09/KMR-2010-0003. Dávid Héja, Péter Gál, Gábor Pál, and Péter Závodszky filed patent application for the SGMI inhibitors.
[S] This article contains supplemental Tables S1–S3 and Figs. S1–S3.
The atomic coordinates and structure factors (codes 3TVJ and 4DJZ) have been deposited in the Protein Data Bank, Research Collaboratory for Structural Bioinformatics, Rutgers University, New Brunswick, NJ (http://www.rcsb.org/).
[1] Both authors contributed equally to this work.
[2] The work of D. H. at EMBL-Hamburg was supported by the EMBO Short Term Fellowship ASTF 2.00-2011.
[3] Supported by a János Bolyai Research Fellowship.
[4] Both authors contributed equally to this work.
[5] To whom correspondence may be addressed. E-mail: gal.peter@ttk.mta.hu.
[6] To whom correspondence may be addressed. E-mail: palgabor@elte.hu.

[7] The abbreviations used are: MBL, mannan-binding lectin (CCP, complement control protein domain); K_i, equilibrium inhibitory constant; MAp19, MBL-associated protein of 19 kDa; MAp44, MBL-associated protein of 44 kDa; MASP, MBL-associated serine protease; PDB, Protein Data Bank; PMP-C, pars intercerebralis major peptide C (a *Locusta migratoria* protease inhibitor); SFMI, SFTI-based MASP inhibitor; SFTI, sunflower trypsin inhibitor; SGPI, *S. gregaria* protease inhibitor; SGMI, SGPI-based MASP inhibitor; SP, serine protease.

three types of recognition molecule-associated proteases designated as MBL-associated serine protease (MASP-1), -2, and -3 (4). Moreover, there are two recognition molecule-associated, non-enzymatic fragments of these proteases, MAp19 and MAp44 (5). MASP-1, MASP-3, and MAp44 are alternative splice products of the *MASP-1/3* gene (6), whereas MASP-2 and MAp19 are that of the *MASP-2* gene (7).

There are many fundamental questions about the activation mechanism and physiological/pathological functions of the lectin pathway. All these could be studied by selective inhibitors. In a recent paper we reported the first MASP-inhibitors developed by directed evolution of the 14-mer sunflower trypsin inhibitor (SFTI) (8). That study led to SFMI-1 (sunflower MASP inhibitor-1) and SFMI-2. SFMI-1 inhibited both MASPs, although it was 15 times less potent against MASP-2 than MASP-1. SFMI-2 was MASP-2-specific. Both peptides turned out to be selective inhibitors of the lectin pathway, but unexpectedly, SFMI-1, the weaker MASP-2 inhibitor, was significantly more potent than SFMI-2. Higher potency of SFMI-1 suggested a significant contribution of MASP-1 to lectin pathway activation. By lacking a monospecific MASP-1 inhibitor, however, we could not quantify the importance of MASP-1.

Here we report the development via directed evolution of truly monospecific and more potent second generation MASP-inhibitors. With these unique reagents we obtained significant new insights in the mechanism of lectin pathway activation and produced the first Michaelis-like complexes for lectin pathway proteases, MASP-1 and MASP-2. MASP-1 has a more open substrate binding cavity and requires only small conformational adjustments upon complex formation. On the other hand, for MASP-2, structural plasticity plays a major role in the substrate binding mechanism.

EXPERIMENTAL PROCEDURES

Reagents—The reagents were from Sigma and Merck. The MaxiSorp plates were from Nunc. The restriction endonucleases and all DNA modifying enzymes were from New England Biolabs and Fermentas.

Construction of SGMI Library—The *Schistocerca gregaria* protease inhibitor (SGPI)-based MASP-inhibitor (SGMI)-library phagemid is based on pKS-Tag-SGCI-p8, which was constructed from pBluescript II KS(−) (Stratagene), pMal-p2X (New England Biolabs), and the M13KO7 helper phage. The vector encodes a periplasmic signal; a FLAG epitope followed by a monovalently displayed SGPI-2 module (9) and the p8 coat protein. The FLAG-tag allows for assessing display bias. The library was produced in two successive mutagenesis steps (10). First, pKS-Tag-SGCI-p8 was used as the template to produce pSGMI-STOP in which all codons to be randomized were replaced with stop codons (underlined) using the primer 5′GCGGTAGCGATGGCAAAAGCGCGTAATGCTAATAATAATAATGCTAACAGGGTACCGGTGGAGG3′. Then pSGMI-STOP was used as template for combinatorial mutagenesis. Stop codons were replaced with NNK degeneracy. N denotes nucleotides A, C, G, or T, and K denotes G or T. NNK codons represent a set of 32 codons covering all 20 amino acids. The mutagenesis primer was 5′GCGGTAGCGATGGCAAAAGCGCGNNKTGCNNKNNKNNKNNKTGCNNKCAGGGTACCGGTGGAGG3′. The phagemid library was electroporated into *Escherichia coli* to generate phage libraries (10).

TABLE 1
Inhibitory potencies of the SGMI-1 and SGMI-2 variants on MASP-1 and MASP-2
Inhibitory potencies are expressed as equilibrium inhibitory constant (K_i) values.

Inhibitor		Sequence (P4-P4′)	K_I MASP-1	K_I MASP-2
			nM	
SGMI-1		FCT**R**KLCY	7	58,000
	$v_{(a)}$[a]	MCT**R**KLCY	14	38,000
	$v_{(b)}$	MCT**R**KLCW	20	6,000
	$v_{(c)}$	ACT**R**KLCW	27	20,000
SFMI-1[b]		ICS**R**SLPP	65	1,030
SGMI-2		VCT**K**LWCN	ND[c]	6
	$v_{(a)}$	VCT**R**LYCN	176 000	32
	$v_{(b)}$	VCT**R**LWCN	87 000	35
	$v_{(c)}$	VCT**R**LWCE	153 000	49
SFMI-2[b]		YCS**R**SYPP	ND[c]	180

[a] Three variants of the highest affinity SGMI-1 and SGMI-2 are denoted as $v_{(a)}$, $v_{(b)}$, and $v_{(c)}$ in descending affinity order.
[b] Data of the published (8) first generation SFTI-based MASP inhibitors SFMI-1 and SFMI-2 are shown for comparison.
[c] No inhibition could be detected even at the highest applied inhibitor concentration.

Preparation of MASP-1 and MASP-2 Catalytic Fragments—Catalytic fragments containing the CCP1-CCP2-SP domains of MASP-1 and MASP-2 were produced as recombinant proteins and purified as described (11, 12). For crystallization of the MASP-2·SGMI-2 complex the CCP2-SP fragment was produced and purified as described (12).

Selection of SGMI Library—MaxiSorp plates were coated with MASP-1, MASP-2, or anti FLAG-tag antibody. The protein concentration was 20 μg/ml for MASPs and 2 μg/ml for the antibody. Three selection rounds were carried out separately on each target, and the binding properties of individual SGMI-phage clones were tested by phage-ELISA (10).

Sequence Analysis—SGMI-phage clones producing an ELISA signal on their target 3-fold above background (measured on BSA containing wells) were sequenced by the Big Dye Terminator v3.1 cycle sequencing kit (Applied Biosystems). To eliminate the effects of display bias, MASP-1- and MASP-2-selected amino acid frequencies were normalized by data from the anti-FLAG-tag selected SGMI-phage population. A dataset of 100 sequences representing the normalized amino acid frequencies at each randomized position was generated and used as the input set for sequence logo generation by the WebLogo program (13).

Expression and Purification of SGMI Variants—SGMI variants were expressed into the periplasm of *E. coli* as maltose-binding protein fusion proteins. The fusion protein was processed, purified to homogeneity, and analyzed by mass spectrometry as described (14).

Inhibitory Constant (K_I) Measurements—Equilibrium inhibitory constants of the SGMI variants listed in Table 1 were determined on MASP-1 and MASP-2 as described (8). Representative plots of K_I measurements are shown in supplemental Fig. S1.

Crystallographic Studies of MASP-2·SGMI-2 and MASP-1·SGMI-1 Complexes—The recombinant CCP2-SP fragment of MASP-2 and SGMI-2 was co-crystallized by the hanging-drop method at 20 °C by mixing 2–3 μl of protein solution (3.3

mg/ml protein complex of 1:1 MASP-2·SGMI-2 molar ratio, 179 mM NaCl, 0.3 mM EDTA, and 3 mM Tris-HCl, pH 7.4, and 2 μl of reservoir solution (24.5% (w/v) PEG 5000 monomethyl ether, 0.164 M $(NH_4)_2SO_4$, and 82 mM MES, pH 6.5). After 30 s of drying, the crystals were flash-cooled and stored in liquid nitrogen. Diffraction data were collected at the European Synchrotron Radiation Facility, Grenoble at beamline ID 14-1 at 100 K (wavelength, 0.9334 Å) from a single crystal by helical data collection. The data were processed and scaled to a resolution of 1.28 Å using the programs XDS and XSCALE (15). The phase problem was solved by molecular replacement using the program MOLREP (16) of the Collaborative Computing Project 4 (17) with individual domains of the MASP-2 structure (PDB ID 1Q3X) and PMP-C structure (PDB ID 1GL1) as search models.

The recombinant CCP1-CCP2-SP fragment of MASP-1 and the SGMI-1 inhibitor were mixed in a 2:3 molar ratio and concentrated to 5 mg/ml. Crystals were obtained by submitting a mix of 1 μl of protein and 1 μl of reservoir solution comprising 0.1 M HEPES, pH 7.0, 25% PEG 1000, 0.3 M $NaNO_3$, to hanging drop vapor diffusion at 20 °C. X-ray data were collected at ID23-1 at European Synchrotron Radiation Facility, Grenoble at 100 K (wavelength, 0.97942 Å). The data were processed with XDS (18) and scaled with SCALA (19). The structure of the MASP-1·SGMI-1 complex was solved by molecular replacement using PHASER (20) with MASP-1 (PDB ID 3GOV) and a bovine trypsin·SGPI-1 complex (PDB ID 2XTT) as search models. The asymmetric unit contains two MASP-1·SGMI-1 complexes. For both structures model building was carried out with the program Coot (21). Both models were refined with Refmac (22) using restrained maximum-likelihood refinement and TLS refinement (23) (TLS groups were defined for the domains of MASP-1 and MASP-2 and for the inhibitors). Individual anisotropic atomic displacement parameters for the MASP-2·SGMI-2 complex were refined and riding hydrogen atoms were added to the structure. Non-crystallographic restraints were applied to domains of MASP-1 and SGMI-1. The models were validated using PROCHECK (24), SFCHECK (25), and MolProbity (26). Data collection and refinement statistics are shown in Table 2. Coordinates were deposited with PDB under reference code 3TVJ and 4DJZ. Analysis of the contact regions was carried out with the CCP4 program and the PISA server (27). Structural figures were prepared by PyMOL (28).

TABLE 2
Crystallographic data collection and refinement statistics

	MASP-2·SGMI-2 complex[a]	MASP-1·SGMI-1 complex[a]
Data collection		
Space group	$P2_12_12_1$	$P2_12_12_1$
Cell dimensions *a*, *b*, *c* (Å)	50.92, 62.47, 114.19	71.33, 98.40, 155.53
Resolution (Å)	39.55-1.28 (1.30-1.28)	46.91-3.20 (3.37-3.20)
R_{meas}[b]	0.065 (0.752)	0.258 (0.997)
$I/\sigma I$	15.10 (2.54)	7.6 (2.3)
Completeness (%)	95.8 (93.3)	99.9 (100.0)
Redundancy	5.44 (5.06)	6.8 (7.1)
Refinement		
Resolution (Å)	38.00-1.28	46.91-3.20
No. reflections	85,991	18,639
R_{work}/R_{free}[c]	0.156/0.205	0.228/0.274
No. atoms		
Protein	2911	6463
Ligand/ion	5	
Water	534	2
B-Factors (Å^2)		
Protein	17.14	47.19
Ligand/ion	18.03	
Water	36.83	11.65
Root mean square deviation		
Bond lengths (Å)	0.025	0.006
Bond angles (°)	2.059	1.036
Ramachandran plot[d]	269/27/2	629/95/1
Molprobity score	1.56	2.62

[a] One crystal was used for data collection. Values in parentheses are for highest resolution shell.
[b] $R_{meas} = \Sigma_{hl}[n_h/(n_h - 1)]^{1/2}|I_{hl} - \langle I_h\rangle|/\Sigma_{hl}\langle I_h\rangle$, where n_h is the number of observations of reflection *h*.
[c] $R = \Sigma_h|F_o - F_c|/\Sigma_h F_o$, $R_{work} = R_{factor}$ for reflection included in refinement calculations, $R_{free} = R$ factor for a selected subset (5%) of the reflections that was not included in refinement calculations.
[d] Number of residues in most favored/allowed/disallowed regions.

RESULTS

Selection of Small Protein Inhibitors against MASP-1 and MASP-2 by Phage Display

We evolved second generation high affinity, high specificity MASP-1 and MASP-2 inhibitors. An inhibitor-phage library was constructed on the scaffold of the reversible serine protease inhibitor SGPI-2 (*S. gregaria* protease inhibitor-2) belonging to the Pacifastin family of canonical inhibitors (Fig. 1*A*) (9, 14, 29–31) to yield SGMI (SGPI-2 based MASP inhibitor) variants. We fully randomized six positions P4, P2, P1, P1′, P2′, and P4′ (according to Schechter and Berger (32)) of the protease binding loop while keeping the structurally indispensable Cys at P3 and P3′ (Fig. 1*A*). The library of 2×10^9 clones was selected on MASP-1, MASP-2, and an anti-FLAG-tag antibody. This latter was used to assess display bias as described under "Experimental Procedures." Clones from the third selection cycle were sequenced.

Selected Inhibitor Variants Reveal Characteristic MASP-specific Binding Loop Sequence Patterns

Based on DNA sequencing, 43 of 48 MASP-1 binders, 30 of 40 MASP-2 binders, and 61 of 63 anti-FLAG-tag mAb binders were unique (supplemental Table S1). The MASP-1- and MASP-2-selected sequence patterns are illustrated as display-bias normalized (see "Experimental Procedures") sequence logos (13) shown on Fig. 1 *B* and *C*.

Phage Display-evolved Variants Are High Affinity, Monospecific MASP Inhibitors

In phage display studies normalized amino acid frequencies correlate with binding energy contributions of amino acid residues (33–37). We designed 4 SGMI-1 and 4 SGMI-2 inhibitor variants (see Table 1) derived from the MASP-1- and MASP-2-selected sequence patterns. One of the four variants was the selected consensus, whereas the others were single point mutants of the consensus or of each other. Mutations represented second or third most preferred residue types. The eight inhibitors were expressed in *E. coli* and purified to homogeneity, and their equilibrium inhibitory constants (K_I) against MASP-1 and MASP-2 were determined (Table 1). The highest affinity MASP-1 and MASP-2 inhibitors were named SGMI-1 and SGMI-2, respectively, whereas their variants in descending affinity order were named SGMI-1v(a, b, c) and SGMI-2v(a, b, c).

The 7-nanomolar MASP-1 inhibitor SGMI-1 is practically monospecific being 8300-fold less effective on MASP-2. Its

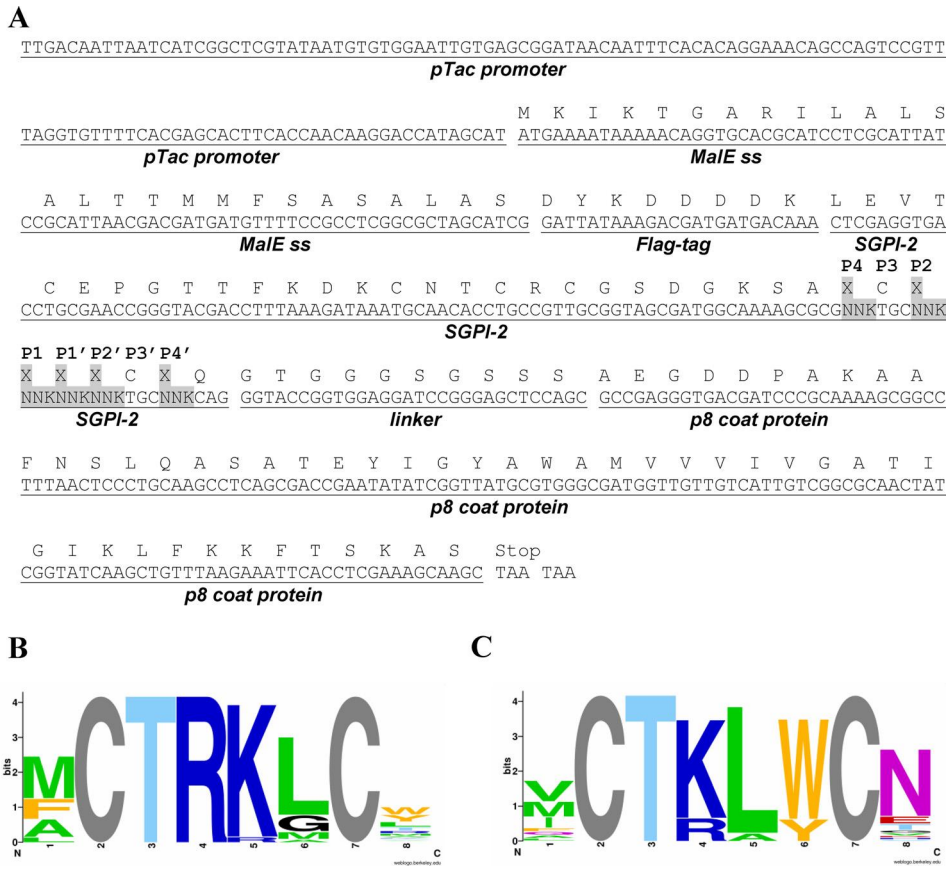

FIGURE 1. **The inhibitor-phage library construct and the results of the MASP-1 and MASP-2 selections are illustrated as sequence logos.** *Panel A* shows the inhibitor-phage library construct. Inhibitor variants flanked by an N-terminal epitope tag (*Flag-tag*) are fused to the p8 coat protein through a Gly/Ser linker. The MalE signal sequence (*MalE ss*) targets the variants to the periplasm before getting incorporated in the phage coat. The fusion gene is controlled by the pTac promoter. Randomized positions in the protease binding loop between the P4-P4′ sites are *highlighted* with *gray*. At these positions all 20 amino acids (*X*) were allowed to occur by using NNK triplets and combinatorial site-directed mutagenesis. From the same library 43 unique MASP-1 and 30 unique MASP-2 binders were selected (listed in supplemental Table S1). These sequences were used to generate display bias normalized (see in "Experimental Procedures") MASP-1 (*B*)- and MASP-2 (*C*)-specific sequence logos. Position heights represent the degree of conservation. Letter heights indicate normalized amino acid frequencies. The two nonrandomized Cys residues in *gray* show maximum height. Other colors indicate chemical properties of the amino acid groups. The P4-P4′ positions are numbered from 1 to 8; therefore, position 4 stands for the P1 site.

SGMI-1v(a, b, c) variants are 2–4-fold less potent and 3–30-fold less selective.

The 6-nanomolar MASP-2 inhibitor SGMI-2 representing the selected consensus is monospecific, having no measurable effect on MASP-1. The SGMI-2 v(a, b, c) variants are 5–8-fold less potent on MASP-2 and are also less selective, being 2500–5500-fold less potent against MASP-1 than MASP-2.

Both SGMI-1 and SGMI-2 Are Selective Lectin Pathway Inhibitors

The Wieslab COMPL 300 assay selectively measures the activation of the three different complement pathways (38). We applied this assay to test the inhibitory properties of SGMI-1 and SGMI-2 on the activation of each complement pathway. While a more complete description of the results is published elsewhere,[8] we note that at 1 μM concentration both SGMI-1 and SGMI-2 completely blocked the lectin pathway activation while leaving the classical and alternative routes unaffected.

[8] Héja, D., Kocsis, A., Dobó, J., Szilágyi, K., Szász, R., Závodszky, P., Pál, G., and Gál, P. (2012) A revised mechanism of complement lectin pathway activation reveals the role of MASP-1 as the exclusive activator of MASP-2. *Proc. Natl. Acad. Sci. U.S.A.* 10.1073/pnas.1202588109.

First Michaelis-like Complexes of Lectin Pathway Proteases

Unlike Structure of MASP-1·SGMI-1 Complex, MASP-2·SGMI-2 Complex Supports Induced Fit or Conformational Selection Substrate-binding Model—All previous MASP structures contained the enzyme in uncomplexed form (11, 39) with the substrate binding cleft partially obscured, hindering accurate description of the substrate binding machinery.

We present the 1.28 Å resolution structure of the active catalytic fragment of MASP-2 in complex with the substrate-like SGMI-2 inhibitor (Fig. 2, *A* and *B*; PDB ID code 3TVJ). The structure represents a Michaelis-like complex revealing the active site of the enzyme and the primary binding loop of the inhibitor in canonical configuration. While there is a typical interaction network at the active site, additional contact regions extend over the canonical binding region. This phenomenon is coupled to significant conformation changes both in MASP-2 and SGMI-2 (see the next sections). We note that only transient kinetic analyses can decide whether the observed conformational changes are generated by an induced fit or a fluctuation fit mechanism (40, 41).

The 3.2 Å resolution structure of the MASP-1·SGMI-1 complex (Fig. 2, *C* and *D*; PDB ID 4DJZ, electron density map is

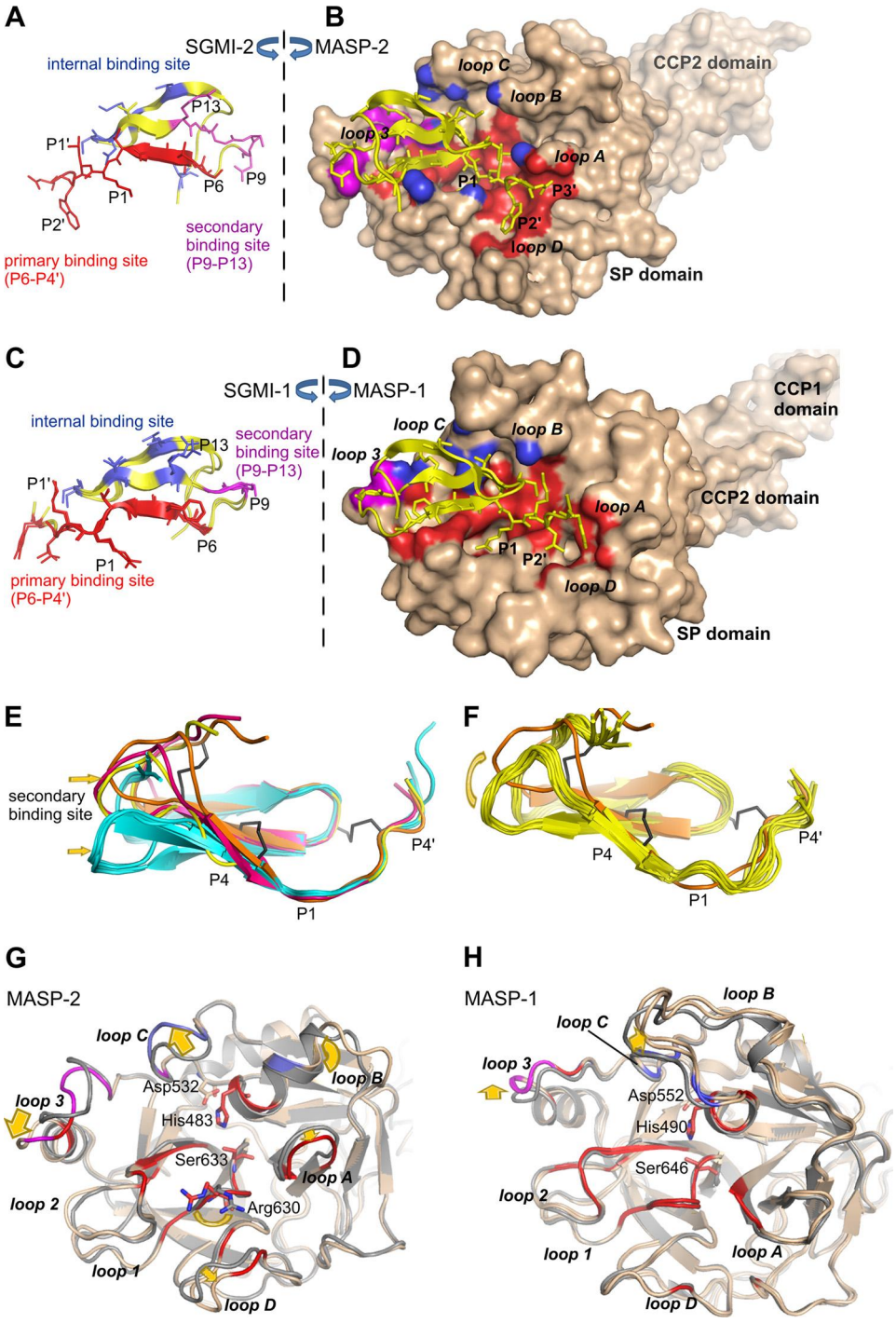

FIGURE 2. **The MASP-2·SGMI-2 and the MASP-1·SGMI-1 structures show extended contact regions and characteristic conformational changes.** In the MASP-2·SGMI-2 complex contacting residues of SGMI-2 (*A*) and MASP-2 (*B*) are shown color-coded (PDB ID 3TVJ). Binding segments of the inhibitor and their binding sites are: *red*, primary; *magenta*, secondary; *blue*, internal binding region. Residues are labeled according to Schechter and Berger (32). Contacting regions of SGMI-1 (*C*) and MASP-1 (*D*) in their complex structure are color-coded as in *A* and *B*. *Panels E* and *F* show comparisons of the complexed SGMI structures with related structures. *E*, SGMI-2 (*orange*) and SGMI-1 (*magenta*) are more distorted than related group-II (*yellow*; PDB ID 1GL1) and group-I (*cyan*, PDB IDs 1GL0, 2XTT, 2VU8, and 2F91) Pacifastin inhibitors in their complexed form. *F*, complex formation distorts the structure of SGMI-2 (*orange*) compared with the free form of its parental molecule, SGPI-2 (*yellow*; PDB ID 1KGM). Conformational changes of MASP-2 and MASP-1 upon complex formation are shown in *G* and *H*, respectively (the uncomplexed form is shown in *gray* for reference). Loops are labeled according to Perona and Craik (45). Residues of the catalytic triad and Arg-630 of MASP-2 are shown in *sticks*. Note, the MASP-1·SGMI-1 structure contains two complexes in the asymmetric unit in similar conformations, both shown in *C* and *H*.

shown in supplemental Fig. S2) also demonstrates an extended binding region, but it is not coupled to any significant distortion in the overall conformation of MASP-1 or SGMI-1.

Extended Binding Site Interactions Form Large Binding Interfaces in Both MASP·SGMI Complexes—In addition to the canonical (primary) binding site (residues 25–34, P5-P5′) Paci-

fastin family inhibitors can possess two other ones. The secondary binding region preceding the canonical sequence is a sharp turn (residues 20–22), whereas the internal binding region is formed by isolated residues on one face of the inhibitor.

Previous studies have shown that these additional sites function only in group-I Pacifastin inhibitors (31, 42–44) and not in group-II inhibitors where SGPI-2, the parent molecule of the SGMIs belongs. In fact, the only known exceptions are the SGMIs, which bind to MASPs with all three binding segments (binding regions are shown in Fig. 2, *A* and *B*, for MASP-2·SGMI-2 complex and Fig. 2, *C* and *D*, for MASP-1·SGMI-1 complex, respectively).

High resolution of the MASP-2·SGMI-2 structure allows for a complete accurate description of the interactions. The combined area of the three binding sites on SGMI-2 is 1107 Å^2, representing the largest interface ever observed for a Pacifastin complex. It is 40% larger than typical (715–884 Å^2) Pacifastin interfaces. The buried surface area within the complex, 2440 Å^2, is also the largest one. The contact interface for the MASP-1·SGMI-1 complex is similarly large (supplemental Table S2).

The secondary binding region of SGMI-2 is more extended (18–22 instead of 20–22) than in other related inhibitors. It forms a contiguous interface interacting with and inducing major rearrangement in loop 3 of MASP-2 (loops are labeled as defined in Perona and Craik (45)) (see below).

Extended Binding Site Interactions Result in Bending of SGMI-2—When a secondary binding region interacts with the protease, it binds at the concave edge of the substrate binding groove, which can promote bending of the inhibitor.

SGMI-2 has the most bent Pacifastin structure hitherto observed (Fig. 2*E*). Comparison of backbone torsion angles and intramolecular hydrogen bonds of SGMI-2 and its close relative, PMP-C (PDB ID 1GL1 (42)), from their complexes suggests that distortion of SGMI-2 is caused by extended interactions with MASP-2 (supplemental Table S3).

SGMI-2 and its parent molecule SGPI-2 differ in only five canonical loop residues. Comparison of the solution structure of SGPI-2 with the bound form of SGMI-2 can therefore model, the conformational changes required in SGMI-2 for binding to MASP-2 (Fig. 2*F*). The comparison suggests a significant distortion upon complexation including major conformational changes at both edges of the secondary binding segment. This distortion might be associated with a binding free enthalpy penalty that lessens the affinity of the interaction. As shown in supplemental Fig. S3, only few stabilizing interactions are identified through the secondary binding segment.

Backbone conformation changes are also detected at residues involved in correct positioning of the P1 residue at the active site (residues 29, 31, and 15; supplemental Table S3). All these changes suggest an induced fit or conformational selection mechanism of inhibitor binding. Similar, but lower level conformational adjustments at these two regions were reported for the group-I SGPI-1 binding to crayfish trypsin (44).

Extended Binding Site Interactions Cause Large Conformational Changes in MASP-2 but Not in MASP-1—All MASP-2 loops carrying inhibitor contacting residues change their conformation during complex formation (Fig. 2*G*). With a few exceptions listed in the next section, enzyme regions contacting the primary binding segment of the inhibitor undergo only minor backbone conformational changes. In the primary binding region of the inhibitor all but two contacts are formed through evolved residues and the backbone of four non-evolved residues. Apparently, topologically focused directed evolution resulted in an optimized primary binding site that ensures high local complementarity to the free structure of MASP-2.

In contrast, loop 3 (residues 602–611) of MASP-2 forming a binding site for the non-evolved secondary binding section and loop C (residues 526–529) of MASP-2 forming a binding site for the non-evolved internal binding region undergo major conformational rearrangements (Fig. 2*G*).

In contrast, in the MASP-1·SGMI-1 complex, distortion of the overall conformation of loop regions is negligible; loop 3 undergoes only a minor shift (Fig. 2*H*), and bending of the inhibitor is similar to that of PMP-C in complex with the inhibited protease (Fig. 2*E*). A possible reason for that is the significantly more open substrate-binding groove of MASP-1. This groove is lined by a shorter loop 3 that appears to contribute to the lower selectivity of MASP-1 for protein substrates.

Conformational Changes Observed at the Primary Substrate-binding Site—The canonical P4-P4′ binding segments on SGMI-1 and SGMI-2 were evolved to bind MASP-1 and MASP-2, respectively, with high affinity. The interactions of this segment on SGMI-2 with MASP-2 are shown in Fig. 3*A*. As mentioned, most binding regions contacting this segment undergo only small, adjusting conformational shifts. Nevertheless, there are three important exceptions. The two in the MASP-2·SGMI-2 complex are as follows. (i) The MASP-2 Arg-630 side chain in the uncomplexed enzyme interferes with the S2′ site and needs to undergo a major conformational change upon complex formation (Fig. 2*G*). A similar change should occur upon complex formation with natural substrates. (ii) The MASP-2 Gln-665 side chain turns inside the enzyme upon complex formation. This conformational change is caused by a shift of Tyr-602 and Tyr-607 upon binding the secondary binding loop (Fig. 3*C*). As this loop is characteristic to the Pacifastin family, this conformational change might not be relevant for all MASP-2 complexes. In fact, as explained below, different conformational changes in the two enzymes explain why and how the Pacifastin scaffold can distinguish MASP-2 and MASP-1 in terms of the optimal P1 residue.

Primary Substrate-binding Site Interactions Explain the Two Different Evolved Sequence Patterns

Interactions through P1 Residue—On small peptide substrates MASP-2 slightly prefers a P1 Arg over Lys (12) yet it selected SGMI-2 variants with a dominance of P1 Lys over Arg. In the complex, Gln-665 forms a hydrogen bond with the S1 Asp-627, affecting the hydrogen bond network of the S1 pocket (Fig. 3*C*). In this network the P1 Lys of SGMI-2 is in a central position participating in several hydrogen bonds, some mediated by a water molecule. Replacing the P1 Lys (and as a consequence the water molecule) with an Arg could result in a direct bivalent hydrogen bonding of Arg to Asp-627 and Gln-665 without perturbing the hydrogen bond network. This could explain why SGMI-2 variants with either P1 Lys or Arg are

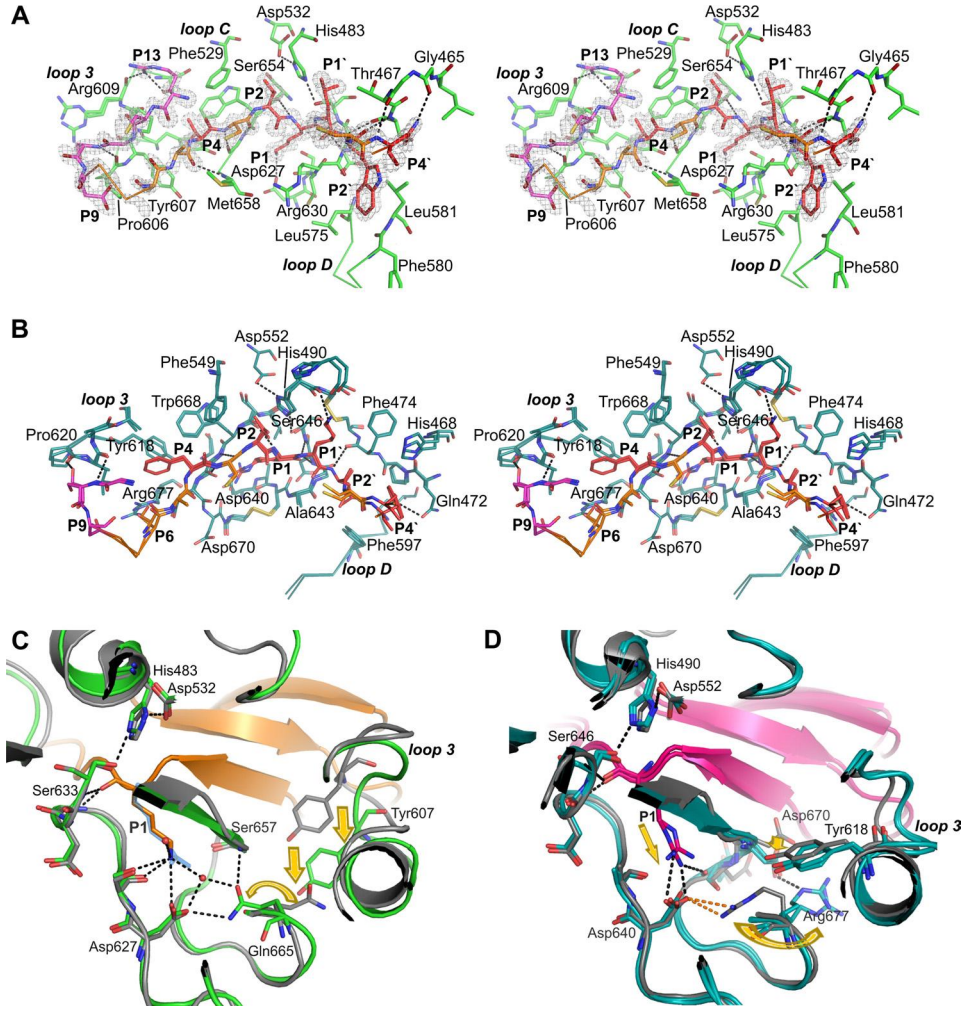

FIGURE 3. **Enzyme/inhibitor interactions in the MASP-2·SGMI-2 and the MASP-1·SGMI-1 structures.** *A*, accommodation of SGMI-2 (*red*, evolved segment; *magenta*, secondary binding segment) in the substrate binding groove of MASP-2 (*green*) is shown in stereo view. $F_o - F_c$ omit map for the P13-P4′ region of the inhibitor is contoured at 4 σ in *gray* (*B*); accommodation of SGMI-1 (*red*, evolved segment; *magenta*, secondary binding segment) in the substrate binding groove of MASP-1 (*cyan*) is shown in stereo view. *C*, the S1 substrate binding pocket of MASP-2 (*green*) is affected by conformational changes induced by the interaction of SGMI-2 (*orange*) and loop 3 of MASP-2. Uncomplexed MASP-2 is shown in *gray* for reference (PDB ID 1Q3X). Modeled P1 Arg (*blue*) is shown in hydrogen-bonding distance from Gln-665. In contrast, in MASP-1, binding of loop 3 has only a minor effect on the S1 site (*D*); however, binding of P1 arginine of the inhibitor (*red*) induces removal of the competing arginine of the enzyme (*cyan*) from the S1 site. Uncomplexed MASP-1 is shown as reference (*gray*; PDB ID 3GOV).

potent MASP-2 inhibitors (see the logo in Fig. 1 and affinities in Table 1).

MASP-1 is strictly P1 Arg-selective (12), and directed evolution exclusively selected a P1 Arg. In contrast to MASP-2, in the case of MASP-1, an Arg to Lys change at the P1 site should cause a dramatic drop of the inhibitory affinity. Comparison of the uncomplexed and complexed forms of MASP-1 (PDB IDs 3GOV (11) and 4DJZ) can explain the different P1 preference of this enzyme. In MASP-1, Arg-677 corresponds to Gln-665 in MASP-2 (11). In uncomplexed MASP-1, Arg-677 faces inside, forming a self-inhibitory salt bridge with the S1 Asp. The P1 Arg or Lys of the substrate or inhibitor should compete with Arg-677 for binding to S1 Asp. Apparently, only the longer/better fitting P1 Arg is an efficient competitor. The MASP-1·SGMI-1 structure supports this hypothesis; Arg-677 is turned out from the S1 pocket, and P1 Arg of SGMI-1 is the only electrostatic partner of the S1 Asp (Fig. 3*D*).

Interactions through Other Evolved Residues—The two MASPs selected highly different patterns. The only exception is the commonly selected wild type Thr at the P2 position, which is strictly conserved in the Pacifastin family (29). At this position directed evolution recapitulated natural evolution. NMR and x-ray structures demonstrated that this Thr participates in a binding loop-stabilizing hydrogen bond network (42, 46–48).

In both MASPs a small binding site is formed for the P2 Thr by adjusting the position of a phenylalanine. Invariant selection of a P2 Thr in SGMI-1 and SGMI-2 is due to the canonical binding loop stabilizing role of the P2 Thr and the highly similar S2 pockets of the two enzymes (Fig. 3, *A* and *B*).

At the less conserved P4 position the two enzymes selected different sets of apolar residues. In both enzymes formation of a small, non-polar S4 pocket by loop 3 is induced by inhibitor binding. Loop 3 folds around the P4 residue and restricts its size. Different sizes and polarities of loop 3 segments in the two enzymes explain the different P4 preferences.

MASP-2 almost exclusively selected a P1′ Leu, which binds in a hydrophobic S1′ site on the enzyme. In contrast, MASP-1 exclusively selected a P1′ Lys, which is also located in a hydro-

phobic S1′ site but is further stabilized by hydrogen-bonding to enzyme backbone oxygen atoms. In the case of MASP-1, a P1′ Leu would clash with the 475–491 disulfide bridge.

At the P2′ position MASP-1 selected aliphatic residues, dominantly Leu, whereas MASP-2 selected only Trp or Tyr. In both enzymes a hydrophobic S2′ site is formed by loop D. The S2′ site of MASP-2 is large but shallow, preferring aromatic P2′ residues, whereas the homolog MASP-1 site accommodates only smaller side chains (Fig. 3, *A* and *B*).

Finally, different sizes and compositions of loop A determines different P4′ preferences of the two enzymes. At the P4′ position MASP-1 preferred apolar, whereas MASP-2 preferred polar residues. The P4′ Asn of SGMI-2 is stabilized by a hydrogen bond network formed with loop A of MASP-2 (Fig. 3*A*). The P4′ Tyr of SGMI-1 is located in a wider binding pocket and interacts with polar and hydrophobic residues (Fig. 3*B*).

DISCUSSION

MASP-1 and MASP-2 have no exclusive natural substrates or inhibitors of their own. MASP-1 shares C2 with MASP-2 and C1s, whereas it shares its other substrates fibrinogen, factor XIII and the PAR-4 receptor with thrombin (12, 49, 50). The more selective MASP-2, which in addition to C2 cleaves only C4, shares this latter substrate with C1s (51). Moreover, the substrate-like serpin-type C1 inhibitor inhibits MASP-1, MASP-2, C1s, C1r, factors XIa and XIIa and plasma kallikrein (52).

It was, therefore, unlikely that based on a substrate-like inhibitor scaffold, monospecific MASP-1 and MASP-2 inhibitors could be evolved. In a previous study we already demonstrated that highly selective MASP-2 inhibitors can be evolved on an SFTI scaffold, but we could not evolve a selective MASP-1 inhibitor (8).

In this study using the larger SGPI scaffold the evolution led to an enzyme-selective and extreme reduction of combinatorial sequence space at the 4 central loop positions P2-P2′. Of the 20^4 = 160,000 combinations, only 8 were selected by both enzymes. At the two outermost positions, P4 and P4′ preferences were less pronounced but still enzyme-specific.

Indeed, based on these patterns, we produced SGMI-1 and SGMI-2, a pair of monospecific MASP-1 and MASP-2 inhibitors, respectively. Through these inhibitors we have shown that the protease domains of both MASP-1 and MASP-2 have unique binding surfaces with a previously hidden, unexpected capacity of monospecific molecular recognition. This suggests that even small molecules might selectively inhibit MASP-1 and MASP-2, opening new opportunities for selective drug development.

Using these monospecific inhibitors as unique research tools, we obtained significant new insights in the relative functional importance of MASP-1 and MASP-2 in lectin pathway activation. Moreover, we also solved the first Michaelis-like complexes of the two enzymes, leading to a better understanding of the differing modes of binding partner recognition by the two MASPs.

In terms of structural insights we found that loop plasticity facilitates MASP-2 binding to inhibitor segments not evolved to interact with the enzyme. Apparently, MASP-2 can adjust its structure to macromolecular substrates using binding elements outside the canonical binding groove. Natural substrates of MASP-2 differ at their P4-P3′ regions and yet, MASP-2 recognizes them highly selectively. The observed loop plasticity could play a major role in that selective recognition and as explained below, the same interactions could induce functionally important conformational changes in or require such changes from the selective substrates. A similar structural accommodation was not observed with MASP-1 having a significantly more open substrate-binding groove and shorter loop3 than MASP-2. We also showed that high level structural plasticity of both partners was required for MASP-2 binding the substrate-like SGMI-2.

Natural substrates of MASP-2, C2 and C4 are highly selective in the sense that only a few additional serine proteases can cleave them. The classical pathway protease C1s cleaves both C2 and C4, whereas MASP-1 cleaves C2.

This remarkable resistance of C2 and C4 against other trypsin-like enzymes suggests that both need to go through functionally relevant conformational changes to become substrates. These changes are either induced, or the productive conformations are stabilized by only upon binding to the adequate protease. The major conformational change observed in the substrate-like SGMI-2 could be an indication of analogous conformational changes induced in natural substrates.

The observed structural plasticity puts MASP-2 among the growing set of complement proteases for which an induced fit mechanism had been suggested, as an analog mechanism of "substrate-induced catalysis" was proposed for the activation of factor D (63), factor B (64), and C2 (65). In fact, it appears that for complement proteases induced fit could be the general mechanism facilitating highly selective substrate recognition.

Our unique Michaelis-like complex structure of MASP-2 also provides an experimental measure on the level of structural plasticity of the enzyme. The structure of both MASP complexes will guide further directed evolution and rational design studies to yield affinity-matured next generation SGMI inhibitors or in fact other unrelated inhibitors. In terms of structural understanding of molecular recognition, it is also noteworthy how directed evolution yielded scaffold dependent optimal sequence patterns of the canonical binding loop.

In a previous study we evolved SFTI-based MASP inhibitors SMFI-1 and SMFI-2 (8). Regardless of whether being selected on MASP-1 or MASP-2, all SFMI inhibitors evolved an identical Ser-Arg-Ser P2-P1-P1′ segment. In contrast, directed evolution on the SGPI-2 scaffold resulted in a different solution at all three analogous positions. This is quite unexpected because the binding loop conformation of reversible inhibitors at the P2-P1-P1′ segment is canonical, *i.e.* practically identical. The differences can be rationalized as follows.

The S2 sites of MASP-2 and MASP-1 are highly similar. A small shift of a Phe is needed to form a more open S2 site facilitating the accommodation of P2 Thr. This Thr is fully conserved in the inhibitor families of SGMIs and SFMIs due to its role in inhibitor structure stabilization. While directed evolution of SGMIs recapitulated natural evolution, for SFMIs it delivered a Ser at this site that is smaller but is still capable to stabilize the inhibitor conformation through hydrogen bond-

ing. Apparently, the smaller SFMI inhibitors do not induce the necessary shift of the Phe residue to accommodate the methyl group of a P2 Thr.

As was shown, the SGPI scaffold allowed for MASP-1/2-selective evolution of a P1 Arg or P1 Lys, respectively, due to an allosteric change of the S1 pocket environment induced by the secondary binding loop. In contrast, the SFTI scaffold invariantly yielded a P1 Arg. The SFTI scaffold lacks any extended binding sites and, therefore, cannot provide any distorting effect on the S1 site. This can explain why the P1 Lys *versus* Arg discrimination did not show up on the SFTI scaffold.

On the SFTI scaffold the P1′ Ser is engaged in an indispensable canonical loop-stabilizing hydrogen bond network. Consequently, this position was selected back as wild type Ser, which is unable to utilize the S1′ site of the enzyme. This notion foretold that different scaffolds not engaging the P1′ for scaffold stabilization should provide room for higher affinity and specificity. Indeed, on the SGPI scaffold MASP-1 and MASP-2 selected highly conserved and very different P1′ residues that should contribute to the great selectivity of SGMI-1 and SGMI-2. All these findings suggest that the present understanding of how reversible serine protease inhibitors function needs to be refined.

In terms of major functional insights we showed that both SGMI-1 and SGMI-2 completely and highly selectively blocked the lectin pathway activation while leaving the classical and alternative routes unaffected. This pathway selectivity means that the SGMIs do not inhibit the classical pathway initiator proteases C1r and C1s, nor C2 or the alternative pathway proteases fB and fD and do not inhibit the C3 and C5 convertases either. MASP-2 is a well established key component of lectin pathway activation (53, 54); therefore, SGMI-2 was expected to completely block the pathway.

On the other hand, MASP-1 had been considered as an auxiliary component, and therefore, its inhibition predicted only partial pathway blockage (55). Yet, to our greatest surprise, the highly selective SGMI-1, which does not inhibit MASP-2, completely arrested the lectin pathway.

This finding clearly shows that MASP-1 is not an auxiliary component. Just like MASP-2, MASP-1 is also an indispensable component of the lectin pathway. In normal human serum without MASP-1 activity, MASP-2 cannot activate the pathway.

This notion is in sharp contrast with previous studies that using either MASP-1-depleted serum (56) or MASP-1 knock-out animals (57) showed that MASP-2 is an autonomous activator of the lectin pathway. We suggest that this apparent discrepancy is due to the non-physiologic nature of the depletion and knock-out experiments.

In our experiment we used normal human serum and *in situ*-acting selective inhibitors. In contrast, MASP-1 depletion or MASP-1 knock-out experiments result in the complete removal of the enzyme from the serum. This allows for filling up its vacancy both in topological as well as in functional terms by other serum components masking the functional importance of the removed MASP-1.

We have conducted carefully designed experiments to pinpoint the exact mechanistic role of MASP-1 in lectin pathway activation to establish a corrected model of the pathway.[8] Without going into details we suggest that in the MASP-1 depletion and knock-out experiments MASP-2 can partially substitute for the missing MASP-1 component.

It was recently shown in animal studies that blocking the lectin pathway by the removal of MASP-2 from the serum either through gene knock-out or antibody-based depletion protects against ischemic reperfusion injury provoked by experimentally induced heart attack (57). This identified MASP-2 as a highly promising therapeutic target. (Note that as MASP-2 can cleave both C2 and C4 while MASP-1 can cleave only C2, MASP-1 cannot substitute for the removed MASP-2 component. Thus, the MASP-2 removing experiments do not generate a substitutable niche for MASP-1). We note that due to its central role identified in this study, MASP-1 is an equally relevant therapeutic target, and both SGMI-1 and SGMI-2 should be promising lead molecules of subsequent drug development.

In recent years the complement system has been recognized as an attractive target for drug development, and much effort has been devoted for developing complement inhibitors. Phage display was used to generate compstatin, a powerful peptide inhibitor that binds to C3 and inhibits the common central step of the complement cascade (58). Another phage display-selected inhibitor is complin, which targets factor B and C2 and consequently inhibits all the three pathways (59). Pathway-selective inhibitors were also developed by interfering with the interaction between the pattern recognition molecules (*e.g.* C1q, MBL) and their targets (60, 61).

Our approach was to selectively block individual serine proteases of the lectin pathway. Previously several attempts had been made to develop low molecular weight inhibitors against complement serine proteases, but those compounds showed low selectivity (62).

Our SGMI-1 and SGMI-2 inhibitors are monospecific, and both are able to selectively arrest the lectin pathway. These inhibitors are invaluable tools for deciphering the mechanism of complement activation and for clarifying the roles played by MASP-1 and MASP-2 in disease models.

Acknowledgments—We acknowledge the European Synchrotron Radiation Facility for provision of synchrotron radiation facilities, and we thank Dr. Stéphanie Monaco and Dr. Sean McSweene for assistance in using beamlines ID14-1 and ID23-1. The authors are grateful to Dr. Miklós Sahin-Tóth for critical reading of the manuscript and for his highly valuable suggestions. G. P. acknowledges László Gráf for initiating the studies on the SGPI inhibitors at the Department of Biochemistry, Eötvös Loránd University in the 1990s.

REFERENCES

1. Ricklin, D., Hajishengallis, G., Yang, K., and Lambris, J. D. (2010) Complement. A key system for immune surveillance and homeostasis. *Nat. Immunol.* **11,** 785–797
2. Thiel, S. (2007) Complement activating soluble pattern recognition molecules with collagen-like regions, mannan binding lectin, ficolins, and associated proteins. *Mol. Immunol.* **44,** 3875–3888
3. Hansen, S., Selman, L., Palaniyar, N., Ziegler, K., Brandt, J., Kliem, A., Jonasson, M., Skjoedt, M. O., Nielsen, O., Hartshorn, K., Jørgensen, T. J., Skjødt, K., and Holmskov, U. (2010) Collectin 11 (CL-11, CL-K1) is a

MASP-1/3-associated plasma collectin with microbial-binding activity. *J. Immunol.* **185,** 6096–6104
4. Gál, P., Dobó, J., Závodszky, P., and Sim, R. B. (2009) Early complement proteases: C1r, C1s, and MASPs. A structural insight into activation and functions. *Mol. Immunol.* **46,** 2745–2752
5. Degn, S. E., Hansen, A. G., Steffensen, R., Jacobsen, C., Jensenius, J. C., and Thiel, S. (2009) MAp44, a human protein associated with pattern recognition molecules of the complement system and regulating the lectin pathway of complement activation. *J. Immunol.* **183,** 7371–7378
6. Skjoedt, M. O., Hummelshoj, T., Palarasah, Y., Honore, C., Koch, C., Skjodt, K., and Garred, P. (2010) A novel mannose-binding lectin/ficolin-associated protein is highly expressed in heart and skeletal muscle tissues and inhibits complement activation. *J. Biol. Chem.* **285,** 8234–8243
7. Fujita, T. (2002) Evolution of the lectin-complement pathway and its role in innate immunity. *Nat. Rev. Immunol.* **2,** 346–353
8. Kocsis, A., Kékesi, K. A., Szász, R., Végh, B. M., Balczer, J., Dobó, J., Závodszky, P., Gál, P., and Pál, G. (2010) Selective inhibition of the lectin pathway of complement with phage display-selected peptides against mannose-binding lectin-associated serine protease-1 (MASP-1) and -2. Significant contribution of MASP-1 to lectin pathway activation. *J. Immunol.* **185,** 4169–4178
9. Szenthe, B., Patthy, A., Gáspári, Z., Kékesi, A. K., Gráf, L., and Pál, G. (2007) When the surface tells what lies beneath. Combinatorial phage-display mutagenesis reveals complex networks of surface-core interactions in the pacifastin protease inhibitor family. *J. Mol. Biol.* **370,** 63–79
10. Sidhu, S. S., Lowman, H. B., Cunningham, B. C., and Wells, J. A. (2000) Phage display for selection of novel binding peptides. *Methods Enzymol.* **328,** 333–363
11. Dobó, J., Harmat, V., Beinrohr, L., Sebestyén, E., Závodszky, P., and Gál, P. (2009) MASP-1, a promiscuous complement protease. Structure of its catalytic region reveals the basis of its broad specificity. *J. Immunol.* **183,** 1207–1214
12. Ambrus, G., Gál, P., Kojima, M., Szilágyi, K., Balczer, J., Antal, J., Gráf, L., Laich, A., Moffatt, B. E., Schwaeble, W., Sim, R. B., and Závodszky, P. (2003) Natural substrates and inhibitors of mannan-binding lectin-associated serine protease-1 and -2. A study on recombinant catalytic fragments. *J. Immunol.* **170,** 1374–1382
13. Crooks, G. E., Hon, G., Chandonia, J. M., and Brenner, S. E. (2004) WebLogo. A sequence logo generator. *Genome Res.* **14,** 1188–1190
14. Szabó, A., Héja, D., Szakács, D., Zboray, K., Kékesi, K. A., Radisky, E. S., Sahin-Tóth, M., and Pál, G. (2011) High affinity small protein inhibitors of human chymotrypsin C (CTRC) selected by phage display reveal unusual preference for P4' acidic residues. *J. Biol. Chem.* **286,** 22535–22545
15. Kabsch, W. (1993) Automatic processing of rotation diffraction data from crystals of initially unknown symmetry and cell constants. *J. Appl. Crystallogr.* **26,** 795–800
16. Vagin, A., and Teplyakov, A. (1997) MOLREP: an Automated Program for Molecular Replacement. *J. Appl. Crystallogr.* **30,** 1022–1025
17. Dodson, E. J., Winn, M., and Ralph, A. (1997) Collaborative Computational Project, number 4. Providing programs for protein crystallography. *Methods Enzymol.* **277,** 620–633
18. Kabsch, W. (2010) XDS. *Acta Crystallogr. D Biol. Crystallogr.* **66,** 125–132
19. Evans, P. R. (1997) *Joint CCP4 and ESF-EAMBC Newsletter on Protein Crytallography* **33,** 22–24
20. Read, R. J. (2001) Pushing the boundaries of molecular replacement with maximum likelihood. *Acta Crystallogr. D Biol. Crystallogr.* **57,** 1373–1382
21. Emsley, P., and Cowtan, K. (2004) Coot. Model-building tools for molecular graphics. *Acta Crystallogr. D Biol. Crystallogr.* **60,** 2126–2132
22. Murshudov, G. N., Vagin, A. A., and Dodson, E. J. (1997) Refinement of macromolecular structures by the maximum-likelihood method. *Acta Crystallogr. D Biol. Crystallogr.* **53,** 240–255
23. Winn, M. D., Isupov, M. N., and Murshudov, G. N. (2001) Use of TLS parameters to model anisotropic displacements in macromolecular refinement. *Acta Crystallogr. D Biol. Crystallogr.* **57,** 122–133
24. Laskowski, R. A., Macarthur, M. W., Moss, D. S., and Thornton, J. M. (1993) PROCHECK: a program to check the stereochemical quality of protein sructures. *J. Appl. Crystallogr.* **26,** 283–291
25. Vaguine, A. A., Richelle, J., and Wodak, S. J. (1999) SFCHECK. A unified set of procedures for evaluating the quality of macromolecular structure-factor data and their agreement with the atomic model. *Acta Crystallogr. D Biol. Crystallogr.* **55,** 191–205
26. Chen, V. B., Arendall, W. B., 3rd, Headd, J. J., Keedy, D. A., Immormino, R. M., Kapral, G. J., Murray, L. W., Richardson, J. S., and Richardson, D. C. (2010) MolProbity. All-atom structure validation for macromolecular crystallography. *Acta Crystallogr. D Biol. Crystallogr.* **66,** 12–21
27. Krissinel, E., and Henrick, K. (2007) Inference of macromolecular assemblies from crystalline state. *J. Mol. Biol.* **372,** 774–797
28. DeLano, W. L. (2002) *The PyMOL Molecular Graphics System,* DeLano Scientific LLC, San Carlos, CA
29. Breugelmans, B., Simonet, G., van Hoef, V., Van Soest, S., and Vanden Broeck, J. (2009) Pacifastin-related peptides. Structural and functional characteristics of a family of serine peptidase inhibitors. *Peptides* **30,** 622–632
30. Malik, Z., Amir, S., Pál, G., Buzás, Z., Várallyay, E., Antal, J., Szilágyi, Z., Vékey, K., Asbóth, B., Patthy, A., and Gráf, L. (1999) Proteinase inhibitors from desert locust, *Schistocerca gregaria*. Engineering of both P(1) and P(1)' residues converts a potent chymotrypsin inhibitor to a potent trypsin inhibitor. *Biochim. Biophys. Acta* **1434,** 143–150
31. Wahlgren, W. Y., Pál, G., Kardos, J., Porrogi, P., Szenthe, B., Patthy, A., Gráf, L., and Katona, G. (2011) The catalytic aspartate is protonated in the Michaelis complex formed between trypsin and an *in vitro* evolved substrate-like inhibitor. A refined mechanism of serine protease action. *J. Biol. Chem.* **286,** 3587–3596
32. Schechter, I., and Berger, A. (1967) On the size of the active site in proteases. I. Papain. *Biochem. Biophys. Res. Commun.* **27,** 157–162
33. Pál, G., Fong, S. Y., Kossiakoff, A. A., and Sidhu, S. S. (2005) Alternative views of functional protein binding epitopes obtained by combinatorial shotgun scanning mutagenesis. *Protein Sci.* **14,** 2405–2413
34. Pál, G., Kouadio, J. L., Artis, D. R., Kossiakoff, A. A., and Sidhu, S. S. (2006) Comprehensive and quantitative mapping of energy landscapes for protein-protein interactions by rapid combinatorial scanning. *J. Biol. Chem.* **281,** 22378–22385
35. Pal, G., Kossiakoff, A. A., and Sidhu, S. S. (2003) The functional binding epitope of a high affinity variant of human growth hormone mapped by shotgun alanine-scanning mutagenesis. Insights into the mechanisms responsible for improved affinity. *J. Mol. Biol.* **332,** 195–204
36. Pál, G., Ultsch, M. H., Clark, K. P., Currell, B., Kossiakoff, A. A., and Sidhu, S. S. (2005) Intramolecular cooperativity in a protein binding site assessed by combinatorial shotgun scanning mutagenesis. *J. Mol. Biol.* **347,** 489–494
37. Weiss, G. A., Watanabe, C. K., Zhong, A., Goddard, A., and Sidhu, S. S. (2000) Rapid mapping of protein functional epitopes by combinatorial alanine scanning. *Proc. Natl. Acad. Sci. U.S.A.* **97,** 8950–8954
38. Seelen, M. A., Roos, A., Wieslander, J., Mollnes, T. E., Sjöholm, A. G., Wurzner, R., Loos, M., Tedesco, F., Sim, R. B., Garred, P., Alexopoulos, E., Turner, M. W., and Daha, M. R. (2005) Functional analysis of the classical, alternative, and MBL pathways of the complement system. Standardization and validation of a simple ELISA. *J. Immunol. Methods* **296,** 187–198
39. Harmat, V., Gál, P., Kardos, J., Szilágyi, K., Ambrus, G., Végh, B., Náray-Szabó, G., and Závodszky, P. (2004) The structure of MBL-associated serine protease-2 reveals that identical substrate specificities of C1s and MASP-2 are realized through different sets of enzyme-substrate interactions. *J. Mol. Biol.* **342,** 1533–1546
40. Koshland, D. E. (1958) Application of a theory of enzyme specificity to protein synthesis. *Proc. Natl. Acad. Sci. U.S.A.* **44,** 98–104
41. Straub, F. B. (1964) Formation of the secondary and tertiary structure of enzymes. *Adv. Enzymol. Relat. Areas Mol. Biol.* **26,** 89–114
42. Roussel, A., Mathieu, M., Dobbs, A., Luu, B., Cambillau, C., and Kellenberger, C. (2001) Complexation of two proteic insect inhibitors to the active site of chymotrypsin suggests decoupled roles for binding and selectivity. *J. Biol. Chem.* **276,** 38893–38898
43. Leone, P., Roussel, A., and Kellenberger, C. (2008) Structure of *Locusta migratoria* protease inhibitor 3 (LMPI-3) in complex with *Fusarium oxysporum* trypsin. *Acta Crystallogr. D Biol. Crystallogr.* **64,** 1165–1171
44. Fodor, K., Harmat, V., Hetényi, C., Kardos, J., Antal, J., Perczel, A., Patthy, A., Katona, G., and Gráf, L. (2005) Extended intermolecular interactions in

a serine protease-canonical inhibitor complex account for strong and highly specific inhibition. *J. Mol. Biol.* **350,** 156–169
45. Perona, J. J., and Craik, C. S. (1997) Evolutionary divergence of substrate specificity within the chymotrypsin-like serine protease fold. *J. Biol. Chem.* **272,** 29987–29990
46. Gáspári, Z., Patthy, A., Gráf, L., and Perczel, A. (2002) Comparative structure analysis of proteinase inhibitors from the desert locust, *Schistocerca gregaria*. *Eur. J. Biochem.* **269,** 527–537
47. Szenthe, B., Gáspári, Z., Nagy, A., Perczel, A., and Gráf, L. (2004) Same fold with different mobility. Backbone dynamics of small protease inhibitors from the desert locust, *Schistocerca gregaria*. *Biochemistry* **43,** 3376–3384
48. Fodor, K., Harmat, V., Neutze, R., Szilágyi, L., Gráf, L., and Katona, G. (2006) Enzyme-substrate hydrogen bond shortening during the acylation phase of serine protease catalysis. *Biochemistry* **45,** 2114–2121
49. Hajela, K., Kojima, M., Ambrus, G., Wong, K. H., Moffatt, B. E., Ferluga, J., Hajela, S., Gál, P., and Sim, R. B. (2002) The biological functions of MBL-associated serine proteases (MASPs). *Immunobiology* **205,** 467–475
50. Megyeri, M., Makó, V., Beinrohr, L., Doleschall, Z., Prohászka, Z., Cervenak, L., Závodszky, P., and Gál, P. (2009) Complement protease MASP-1 activates human endothelial cells. PAR4 activation is a link between complement and endothelial function. *J. Immunol.* **183,** 3409–3416
51. Thiel, S., Vorup-Jensen, T., Stover, C. M., Schwaeble, W., Laursen, S. B., Poulsen, K., Willis, A. C., Eggleton, P., Hansen, S., Holmskov, U., Reid, K. B., and Jensenius, J. C. (1997) A second serine protease associated with mannan-binding lectin that activates complement. *Nature* **386,** 506–510
52. Davis, A. E., 3rd, Lu, F., and Mejia, P. (2010) C1 inhibitor, a multi-functional serine protease inhibitor. *Thromb. Haemost.* **104,** 886–893
53. Vorup-Jensen, T., Petersen, S. V., Hansen, A. G., Poulsen, K., Schwaeble, W., Sim, R. B., Reid, K. B., Davis, S. J., Thiel, S., and Jensenius, J. C. (2000) Distinct pathways of mannan-binding lectin (MBL)- and C1-complex autoactivation revealed by reconstitution of MBL with recombinant MBL-associated serine protease-2. *J. Immunol.* **165,** 2093–2100
54. Chen, C. B., and Wallis, R. (2004) Two mechanisms for mannose-binding protein modulation of the activity of its associated serine proteases. *J. Biol. Chem.* **279,** 26058–26065
55. Takahashi, M., Iwaki, D., Kanno, K., Ishida, Y., Xiong, J., Matsushita, M., Endo, Y., Miura, S., Ishii, N., Sugamura, K., and Fujita, T. (2008) Mannose-binding lectin (MBL)-associated serine protease (MASP)-1 contributes to activation of the lectin complement pathway. *J. Immunol.* **180,** 6132–6138
56. Møller-Kristensen, M., Thiel, S., Sjöholm, A., Matsushita, M., and Jensenius, J. C. (2007) Cooperation between MASP-1 and MASP-2 in the generation of C3 convertase through the MBL pathway. *Int. Immunol.* **19,** 141–149
57. Schwaeble, W. J., Lynch, N. J., Clark, J. E., Marber, M., Samani, N. J., Ali, Y. M., Dudler, T., Parent, B., Lhotta, K., Wallis, R., Farrar, C. A., Sacks, S., Lee, H., Zhang, M., Iwaki, D., Takahashi, M., Fujita, T., Tedford, C. E., and Stover, C. M. (2011) Targeting of mannan-binding lectin-associated serine protease-2 confers protection from myocardial and gastrointestinal ischemia/reperfusion injury. *Proc. Natl. Acad. Sci. U.S.A.* **108,** 7523–7528
58. Qu, H., Magotti, P., Ricklin, D., Wu, E. L., Kourtzelis, I., Wu, Y. Q., Kaznessis, Y. N., and Lambris, J. D. (2011) Novel analogues of the therapeutic complement inhibitor compstatin with significantly improved affinity and potency. *Mol. Immunol.* **48,** 481–489
59. Kadam, A. P., and Sahu, A. (2010) Identification of Complin, a novel complement inhibitor that targets complement proteins factor B and C2. *J. Immunol.* **184,** 7116–7124
60. Roos, A., Nauta, A. J., Broers, D., Faber-Krol, M. C., Trouw, L. A., Drijfhout, J. W., and Daha, M. R. (2001) Specific inhibition of the classical complement pathway by C1q-binding peptides. *J. Immunol.* **167,** 7052–7059
61. Montalto, M. C., Collard, C. D., Buras, J. A., Reenstra, W. R., McClaine, R., Gies, D. R., Rother, R. P., and Stahl, G. L. (2001) A keratin peptide inhibits mannose-binding lectin. *J. Immunol.* **166,** 4148–4153
62. Ricklin, D., and Lambris, J. D. (2007) Complement-targeted therapeutics. *Nature biotechnology* **25,** 1265–1275
63. Volanakis, J. E., and Narayana, S. V. (1996) Complement factor D, a novel serine protease. *Protein Sci.* **5,** 553–564
64. Milder, F. J., Gomes, L., Schouten, A., Janssen, B. J., Huizinga, E. G., Romijn, R. A., Hemrika, W., Roos, A., Daha, M. R., and Gros, P. (2007) Factor B structure provides insights into activation of the central protease of the complement system. *Nat. Struct. Mol. Biol.* **14,** 224–228
65. Milder, F. J., Raaijmakers, H. C., Vandeputte, M. D., Schouten, A., Huizinga, E. G., Romijn, R. A., Hemrika, W., Roos, A., Daha, M. R., and Gros, P. (2006) Structure of complement component C2A. Implications for convertase formation and substrate binding. *Structure* **14,** 1587–1597